Brain Pathology ISSN 1015-6305

RESEARCH ARTICLE

Vascular Degeneration in Parkinson's Disease

Jian Guan[1]; Darja Pavlovic[1,2]; Nicholas Dalkie[2]; Henry J. Waldvogel[2]; Simon J. O'Carroll[2]; Colin R. Green[3]; Louise F.B. Nicholson[2]

[1] Liggins Institute, University of Auckland, Auckland, New Zealand.
[2] Centre for Brain Research, and the Department of Anatomy with Radiology, Faculty of Medicine and Health Science, University of Auckland, Auckland, New Zealand.
[3] Department of Ophthalmology, Faculty of Medicine and Health Science, University of Auckland, Auckland, New Zealand.

Keywords
endothelial clusters, factor VIII, human cases, Parkinson's disease, vascular degeneration.

Corresponding author:
Jian Guan, MD, PhD, The Liggins Institute, the University of Auckland, Private Bag 92019, Auckland 1023, New Zealand
(E-mail: *j.guan@auckland.ac.nz*)

Received 13 July 2012
Accepted 9 August 2012
Published Online Article Accepted 16 August 2012

doi:10.1111/j.1750-3639.2012.00628.x

Abstract

Vascular degeneration plays a significant role in contributing to neurodegenerative conditions such as Alzheimer's disease. Our understanding of the vascular components in Parkinson's disease (PD) is however limited. We have examined the vascular morphology of human brain tissue from both PD and the control cases using immunohistochemical staining and image analysis. The degenerative morphology seen in PD cases included the formation of endothelial cell "clusters," which may be contributed by the fragmentation of capillaries. When compared to the control cases, the capillaries of PDs were less in number ($P < 0.001$), shorter in length ($P < 0.001$) and larger in diameter ($P < 0.01$) with obvious damage to the capillary network evidenced by less branching ($P < 0.001$). The level of degeneration seen in the caudate nucleus was also seen in the age-matched control cases. Vessel degeneration associated with PD was, however, found in multiple brain regions, but particularly in the substantia nigra, middle frontal cortex and brain stem nuclei. The data suggest that vascular degeneration could be an additional contributing factor to the progression of PD. Thus, treatments that prevent vascular degeneration and improve vascular remodeling may be a novel target for the treatment of PD.

INTRODUCTION

Parkinson's disease (PD) is the most common neurodegenerative condition in the aging human population second only to Alzheimer's disease (AD) (7). Neuronal degeneration in both PD and AD has been characterized in human cases (23), providing fundamental information for the establishment of animal models and their use in drug discovery and development for these conditions. In addition to neurodegeneration, the vascular components in AD have recently been identified as a key pathological feature and possible contributing factor to disease progress (38). However, the vascular changes in PD are not known, and this is therefore an important question that needs to be addressed.

The vascular changes in AD and other age-related neurological conditions have been described as degenerative, with a loss of ability in vascular remodeling and/or angiogenesis (21, 26). Neuronal degeneration in PD is thought to start in the substantia nigra (SN), leading to dopamine depletion in the nigro-striatal pathway. The degeneration can spread progressively to other brain regions both within the basal ganglia nuclei, including the caudate nucleus (CN), and the cerebral cortex, particularly the middle frontal gyrus of the cerebral cortex (MFG) (29). PD is however a multisystems disorder marked by a profound but less appreciated cell loss in the locus coeruleus (LC), a nucleus that contains the large pigmented noradrenergic neurons of the brain (3, 16, 28). Lewy bodies, characteristic of PD, are also found in the LC (16, 28). In a study examining the neuronal degeneration in the LC concurrently with that observed in the SN, it was found that not only was the LC affected first in PD but that the greatest cell loss was in the LC suggesting that these two nuclei may share common pathogenetic susceptibilities (37). Interestingly, the median raphe nucleus (RN) appears to be either spared or only mildly affected (12). To the best of our knowledge, there is little known of any accompanying vascular changes in those brain regions where neuronal degeneration has been characterized in PD. Furthermore, a better understanding of the pathology of human disease has now become more critical than previously thought, for example, the contribution of the vascular degeneration to the neuronal degeneration of PD. Using brain tissue collected from both PD cases and the aged-matched controls, we have evaluated the vascular changes in the brain regions known to be affected morphologically in PD.

METHODS

Tissue preparation

Human brain tissue from the Neurological Foundation New Zealand Human Brain Bank was used in this study. The methods used for brain tissue preparation have been published previously (34). Briefly, the brains were perfused through the cerebral arteries with phosphate buffered saline (PBS) containing 1% sodium nitrite for 15 minutes. Following this, the brain was perfused with 15% formalin fixative solution in 0.1 M phosphate buffer for 30–45 minutes. The brain was then placed in the same formalin

fixative solution overnight. Dissection of the brain regions into blocks followed the overnight fixation process. The blocks were then post-fixed for a further 1 to 2 days before being cryoprotected prior to freezing. Cryoprotection was completed by transfer of the blocks sequentially into a 20% and then 30% sucrose solution in 0.1 M phosphate buffer with 0.1% sodium azide. At this point, the blocks were stored at −80°C until required.

Experiment 1

Case selection

Selection of PD cases was completed based on the following selection criteria: a postmortem delay less than 48 h and a pathological diagnosis of idiopathic PD. The pathological diagnosis of idiopathic PD was preferred as this reflects the pathological state of 95% of PD sufferers. The age, sex, postmortem delay, pathological state and cause of death of PD cases and age-matched controls are summarized in Tables 1 and 2, respectively.

Immunohistochemical staining

Three brain regions were used: the central region of the middle frontal gyrus of the cerebral cortex (MFG), the CN of the striatum and the SN. Sequential coronal sections (50 μm) from each of the above regions were cut on a frozen microtome and collected. Sections were stored in PBS-azide at 4°C until use. Sections were selected from PD and control cases. Three sections (every 12th section 600 μm apart) were chosen from each region per case and Von Willebrand-associated factor VIII (factor VIII) immunohistochemistry was used for visualizing blood vessels. The free-floating methodology was employed for immunohistochemical staining; this has been described previously (34).

The selected sections were incubated with PBS and 0.2% Triton-X (PBST) overnight then pretreated with 50% methanol and 1% hydrogen peroxide for 20 minutes. The sections were then washed for 10 minutes in PBST before being incubated with Rabbit-anti factor VIII antibody (1:2000, Dako Corporation, Carpinteria, CA, USA) for 48 h at 4°C. The tissue was then washed in three 10-minute PBST washes and then incubated in biotinylated secondary anti-rabbit antibody (1:2500) for 24 h at room temperature, followed by washes and incubation in ExtrAvidin-HRP for 4 h at room temperature. The tissue was then washed and incubated in a solution of 0.05% 3,3-diaminobenzidine (DAB) with 0.01% hydrogen peroxide in 0.1 M phosphate buffer for15 minutes to give a brown reaction product to visualize the labeled blood vessels.

Sections were then mounted onto glass slides, air-dried, dehydrated through a graded alcohol series and cover-slipped. Negative control staining was generated by omitting the primary antibody.

Image analysis

Images were captured using a digital camera system (Nikon Digital Sight) and stored in the tiff format. ImageJ software (V1.46) was used to measure the vascular structure and morphology in these images. The following parameters were analyzed: (1) total number of blood vessels; (2) total length of blood vessels; (3) total number of vessels that were >50 μm; (4) the number of branches; and (5) the number and the area of the "clusters" in blood vessels. Four images per sample (10 × 10 magnification) were captured from each section of the SN, MFG and CN. Each sample area was approximately 8.325 mm^2. Blood vessel numbers, length and branches were measured using skeletonized binary

Table 1. Clinical information of the 10 PD cases selected for the experiment 1.

Case	Age	Sex	PM delay	Pathologist notes	Cause of death
PD30	82	M	19 h	PD with diffuse cortical Lewy body disease.	Multi-organ failure, multiple strokes.
PD33	91	M	4 h	Idiopathic PD, moderate neuronal loss in the substantia nigra with gliosis and poor pigmentation of remaining neurons.	Pneumonia.
PD34	75	F	10 h	PD Cortical Lewy Body disease. Severe loss of melanin containing neurons and mild gliosis observed in substantia nigra.	Cerebrovascular accident.
PD35	73	M	16 h	PD Cortical Lewy Body disease. Severe loss of pigment neurons and gliosis in the substantia nigra.	Pneumonia.
PD36	78	F	22.5 h	Idiopathic PD, Cerebral amyloid angiopathy. Moderate to marked loss in sections of substantia nigra, mild gliosis.	Bronchopneumonia.
PD37	81	M	4 h	Idiopathic PD, moderate to marked loss of pigmented neurons, mild gliosis, pigment incontinence in substantia nigra and locus coeruleus.	Parkinson's Disease associated complications.
PD39	83	M	4 h	PD and progressive supranuclear palsy and Alzheimer-type changes. Pigmented cells mostly preserved in substantia nigra. Some basophilic tangles and globose morphology observed in the SN neurons.	Bronchopneumonia.
PD42	83	M	21 h	PD-moderate loss of pigmented cells and mild gliosis in the substantia nigra.	Myocardial infarction.
PD46	77	M	34 h	Idiopathic PD, low Lewy body numbers. Lacunar infarct in the caudate nucleus showing neuronal loss.	Bronchopneumonia.
PD48	84	M	Unknown (rcvd fixed)	Idiopathic PD, no sign of spongiform or spongy atrophic changes. SN shows patchy neuronal loss with gliosis.	Not given.

Table 2. Clinical information of the 6 controls selected for the experiment 1.

Case	Age	Sex	PM delay	Pathologist notes	Cause of death
H127	59	F	21 h	No neurological history > normal. (No path report)	Pulmonary embolus.
H137	77	F	12 h	Some amyloid plaques but consistent with age-related change. No significant histological abnormalities.	Coronary atherosclerosis.
H139	73	M	5.5 h	No significant histological abnormalities.	Ischemic heart disease secondary to hypertension.
H152	79	M	18 h	Some amyloid plaques but consistent with age-related change. No cortical or nigral Lewy bodies seen.	Congestive heart failure due to chronic restrictive pericarditis.
H169	81	M	24 h	No evidence of neuronal loss, no neurofibrillary changes and no neuritic plaques. No significant histological abnormalities.	Asphyxia, CO poisoning.
H202	83	M	14 h	No evidence of neuronal loss, no neurofibrillary changes and no neuritic or vascular plaques. No significant changes of a degenerative type found.	Ruptured abdominal aortic aneurysm.

images. These were created in ImageJ by adjusting the images to decrease background and lighten the image. The ImageJ threshold tool was then used to select only the blood vessels and create a binary image. This image was then skeletonized. The "Analyse Skeleton" tool in the Bone J plug-in for ImageJ was then used to obtain measurements of the number of blood vessels, the number of branches and the length of blood vessels in the image. This plug-in works by tagging all of the pixels and voxels in an image and counts all of the junctions, branches and provides both an average and maximum length (2).

In order to measure the clusters observed in vessels, images were lightened using ImageJ. The threshold tool was then used to select the darkest particles in the image and to create a binary image using these. Measurements were completed using the "Analyse Particle" tool that allowed us to count the number of darkly staining particles in the image. The tool also provided information regarding the cluster coverage. The cluster coverage was given as the percentage cover of the area of the image that was occupied by the darkest particles. This information allowed us to measure the difference in the intensity of endothelial staining in PD brain vessels as well as providing information on the number of endothelial clusters observed in PD brains.

Experiment 2

Case selections

The clinical details of the cases used for the second experiment are indicated in Tables 3 and 4 for PD and the non-PD controls, respectively. For all PD cases, the pathological diagnosis included idiopathic PD. For this part of the study, the brain regions SN, LC and RN were analyzed for average diameter of vessels and cross-sectional areas of vessels.

Immunohistochemical staining

Brain regions of SN, LC and RN were stained with factor VIII using the same methodology as described for experiment 1, except that the factor VIII was visualized using florescence conjugated (Alexa Fluor 568) goat anti-rabbit (1:500).

Imaging analysis

Stacks of images were collected on a Leica SP2 confocal scanning laser microscope. Blood vessel size was determined by measuring the average diameter and the cross-sectional area of vessels. The number of blood vessels categorized as either less than or greater than 10 μm in diameter was also determined in all three brain regions of the SN, LC and RN. The ImageJ program was used to calculate the diameter and cross-sectional area of the blood vessels in each brain area of each of the PD and control cases. Since blood vessels ran at a reasonably consistent size and shape through the entire Z-stack, only one slice was chosen for quantification of the properties of blood vessels. Each slice covered an area of 211.97 μm × 211.97 μm; therefore, the total number of vessels and the number of vessels in each size bracket are presented as an average over an area of 44 931 μm^2. The density of vessels/mm^2 was converted for statistical analysis and data presentation.

For the diameter measurements, the "line" tool was used to draw a line from the inside wall of the blood vessel lumen to the opposite side. ImageJ was then able to return a value of the length of this drawn line. A similar protocol was followed for measuring the cross-sectional area of each blood vessel; however, in this instance, the "freehand selection" tool was used to encircle the entire lumen and the program measured the area of the shape drawn. The number of vessels present in the field was counted manually.

Table 3. Clinical information of the 6 PD cases used for experiment 2.

Case	Age	Sex	PM delay	Pathology notes	Cause of death
PD31	67	Male	25 h	Idiopathic PD.	Morphine toxicity/ respiratory failure.
PD21	79	Female	9.5 h	Idiopathic PD, evidence of diffuse amyloid plaques also affecting some parts of the cortex.	Senile debility.
PD23	78	Female	18.5 h	Idiopathic PD. Severe loss of pigmented neurons and gliosis in the substantia nigra, Lewy bodies rare in residual neurons.	Pneumonia 2° UTI & PD.
PD29	79	Male	8 h	Idiopathic PD, some scattered Lewy Bodies seen in some regions.	Not given.
PD32	71	Male	8 h	Idiopathic PD with mild cortical Lewy Body disease.	Ischemic heart disease/ Congestive heart failure.
PD33	91	Male	4 h	Idiopathic PD, 30 years since diagnosis, moderate neuronal loss in the substantia nigra with gliosis and poor pigmentation of remaining neurons.	Pneumonia.

Statistical analysis

The difference between the age-matched control and PD cases was analyzed in different brain regions using a two-way analysis of variance (ANOVA) with brain regions treated as dependent factors. The Bonferroni post-test was used for specific differences between the individual brain regions.

RESULTS

Vascular morphology

Immunopositive staining of factor VIII was evenly distributed in the vessel walls in the age-matched non-PD controls (Figure 1A). The main striking feature of pathological change observed in PD was the presence of "clusters" in the endothelium (Figure 1B) of the blood vessels, where the factor VIII staining was unevenly distributed in the vessels. The staining was almost entirely absent in some parts of the blood vessel, while other areas showed densely stained "clusters" (arrows, Figure 1B) of varying sizes and shapes. The most commonly seen "clusters" were "ladder-like" staining with rungs cross-linked to both sides of the vessel wall. Image analysis showed that the number of "clusters" was significantly higher in the PD cases compared to the age-matched controls.

The "clusters" were evaluated by measuring the number of "clusters" and the total area of densely stained "clusters" per field of view. The data suggest that the number of "clusters" was significantly increased in the PD cases ($n = 10$) compared to the control cases ($n = 6$, $P < 0.0001$, $F = 7.1$ [1,41], Figure 2A). There was no significant difference between the numbers of clusters in the different brain regions examined with the difference between the groups (PD/Controls) being brain region dependent ($P = 0.01$, $F = 4.8$ [2,41], Figure 2A). There was a significant increase in the number of "clusters" in the brain regions of the SN ($P < 0.05$) and CN ($P < 0.001$, Figure 2A), but not the MFG.

Similarly, the difference in the area of "cluster" staining was significantly increased in the PD cases ($n = 10$) compared to the control cases ($n = 6$, $P < 0.0001$, $F = 88.94$ [1,41], Figure 2B). There was a moderate difference between the brain regions ($P = 0.02$, $F = 7.42$ [1,41]) and the difference between the groups was not dependent on the brain regions. The post-test showed a

Table 4. Clinical information of the 4 control cases used in experiment 2.

Case	Age	Sex	PM delay	Pathology notes	Cause of death
H161	72	Male	24 h	No neurological history > normal. (No path report)	Aortic aneurysm
H190	72	Female	19 h	No neurofibrillary tangles, neuritic plaques or cortical Lewy bodies > control specimen	Myocardial infarction
H197	19	Female	Exact time of death unknown. Max 40 h	No significant histological changes	Asphyxiation due to hanging
H211	41	Male	8 h	No significant evidence of degenerative disease	Ischemic heart disease

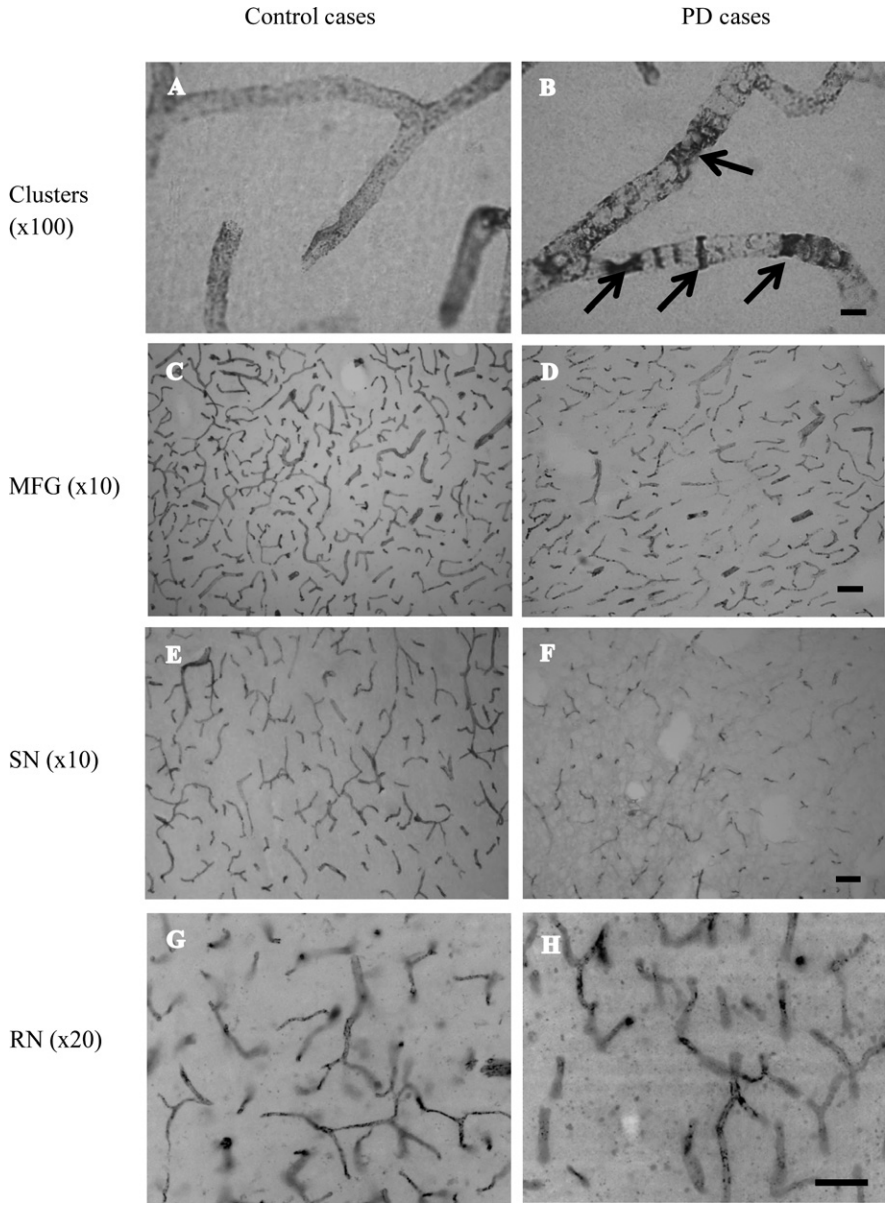

Figure 1. Digital images of endothelial clusters (**A,B**, ×100), the capillaries from the MFG (**C,D**, ×10); SN (**E,F**, ×10); RN (**G,H**, ×20) in PD (right column) and control cases (left column). While the endothelial staining was evenly distributed in the capillaries of the control cases we found a large number of endothelial clusters (arrows) in the PD capillaries (**A,B**). Compared to the control cases, the number of capillaries in PD cases were less and shorter (**C–F**) and had larger diameters (**G,H**). Photos **G,H** are the inverted florescent images. Scale bars = 5 μm for **A** and **B** and 50 μm for **C–H**.

significant increase in the area of "clusters" staining throughout all the brain regions examined ($P < 0.001$, Figure 2B).

Vessel density

The vessels in the PD cases appeared to be fewer in number, shorter and more fragmented (Figure 1D,F) compared to the control cases (Figure 1C,E). The number of vessels/mm^2 was measured in the microscopy field (Figure 3). Compared to the age-matched controls ($n = 6$), the density of blood vessels was significantly decreased in PD cases (Figure 3A, $n = 10$, $P = 0.02$, $F = 5.5$ [1, 41). The two-way ANOVA also suggested a difference between the brain regions ($P < 0.0001$, $F = 26.32$ [2,41], and the reduction in vessel density in PD was brain region dependent ($P < 0.0001$, $F = 13.14$ [1,41). The post-test suggested a significant reduction in vessel density in the SN of PD ($P < 0.001$).

The vessel density of those vessels longer than 50 μm was significantly less in the PD cases compared to that of controls ($n = 10$, $F = 50.99$[1,41], $P < 0.0001$) in the three different brain regions ($F = 16.76$[2,41], $P < 0.0001$) with interaction between them ($F = 10.5$[2,41], $P = 0.0003$). The Bonferroni post-test suggested that the total length of blood vessels in the SN ($P < 0.001$) and MFG ($P < 0.001$) was significantly less in the PD cases compared to the age-matched controls (Figure 3B).

Average vessel length

The average length of the vessels per microscopy area (8.325 mm^2) was measured for the total number of vessels present (Figure 4A)

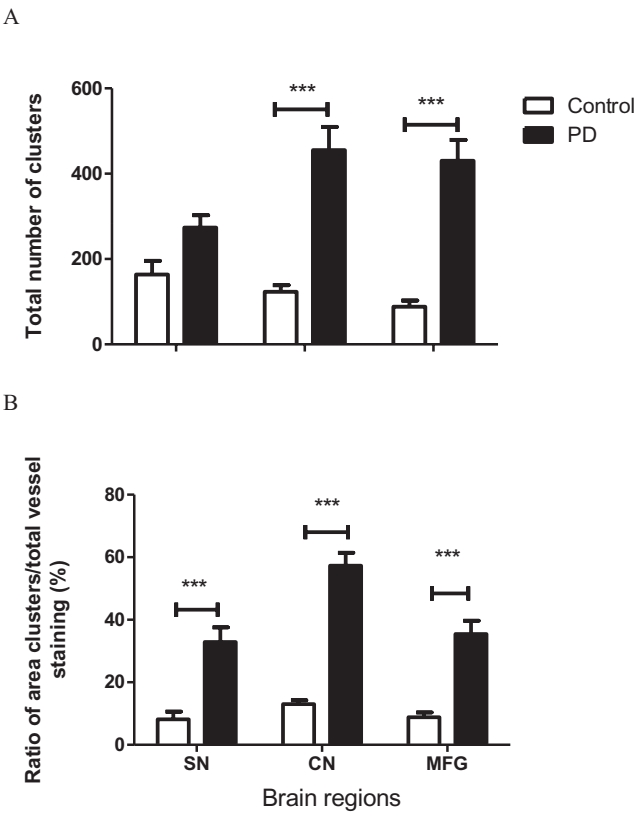

Figure 2. *Graphs show changes in endothelial clusters*. Compared to the age-matched control cases ($n = 6$), the number of endothelial clusters (**A**) and the percentage of vessel area with clusters (**B**) were significantly increased in the SN, CN and MFG of the PD cases ($n = 10$, $^{***}P < 0.001$). Data presented as mean ± SEM.

and for those vessels greater than 50 μm long (Figure 4B). Compared to the age-matched controls ($n = 6$), the average length of all vessels was significantly reduced in PD cases ($n = 10$, $P = 0.01$, F = 6.57 [1,41]). There was also a difference between the brain regions ($P = 0.005$, F = 9.1[2,41]. The difference between the groups was brain region dependent ($P = 0.004$, F = 6.97, [2,41]. The post-test showed that vessel length was significantly shorter in the MFG of PD ($P < 0.001$).

Overall average length of blood vessels >50 μm was also significantly decreased in PD cases ($n = 10$) compared to the age-matched control cases ($n = 6$, $P < 0.0001$, F = 27.19 [1,41], Figure 4B], particularly in the SN ($P < 0.001$) and the MFG ($P < 0.0001$). The total length of blood vessels was different between the brain regions examined ($P < 0.0001$, F = 15.9 [2,41]) with a significant interaction between the brain regions and groups ($P = 0.001$, F = 8.16 [1,41]).

Vessels branches

The two-way ANOVA also showed that PD cases ($n = 10$) had significantly less branching of the blood vessels compared to the control cases ($n = 6$, $P < 0.0001$, F = 18.3 [1,42], Figure 5). The post-test suggested a significant loss in the SN of PD cases compared to the control cases ($P < 0.0001$). There was a significant difference between the brain regions ($P < 0.0001$, F = 22.8 [2,42]) and the difference between the groups was brain region dependent ($P < 0.0001$, F = 18.63 [2,42]).

Vessel width

The vessel width was evaluated in different brain regions in experiment 2. The diameters of the blood vessels were significantly larger in the PD cases ($n = 6$) compared to the control cases ($n = 4$, $P = 0.003$, F = 10.20 [1,24], Figure 6A). There was no difference between the regions examined and the difference between the groups was not brain region dependent. The post-test showed a statistically significant increase in vessel diameters in the RN of PD cases compared to the control cases ($P < 0.05$).

The cross-sectional area of vessels was also significantly increased in the PD cases ($n = 6$) compared to the controls ($n = 4$, $P = 0.01$, F = 7.56 [1,24], Figure 6B) with no difference between the brain regions and the difference between the groups was not brain region dependent. The post-test suggested a significant increase in the cross-sectional area of vessels in the RN of PD cases compared to the control cases ($P < 0.05$).

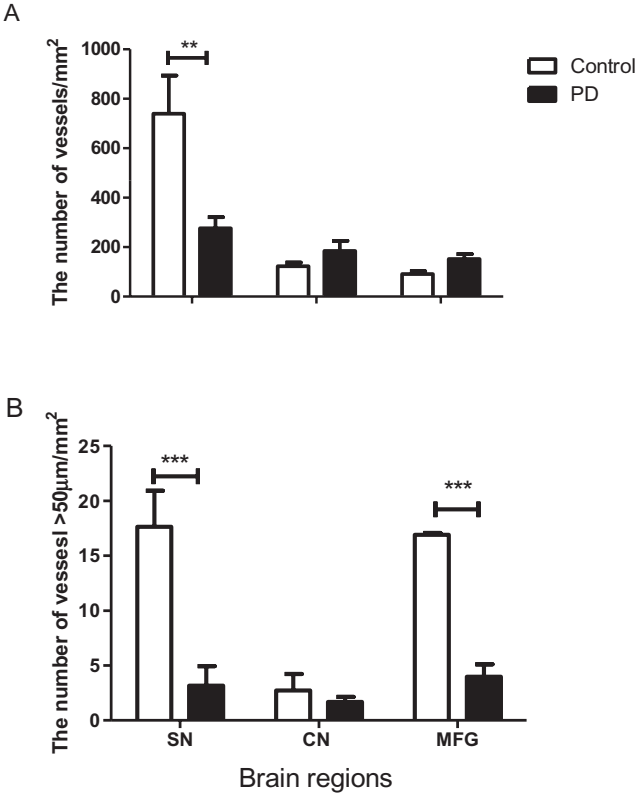

Figure 3. *Graphs show changes in vessel density*. Compared to the age-matched control cases ($n = 6$), the total vessel number was significantly less in the SN of PD cases (**A**, $n = 10$, $^{*}P < 0.01$), but not in the CN and MFG. The number of vessels that were longer than 50 μm were significantly less in the SN and MFG of the PD cases compared to the control cases (**B**, $^{***}P < 0.001$). Data presented as mean ± SEM.

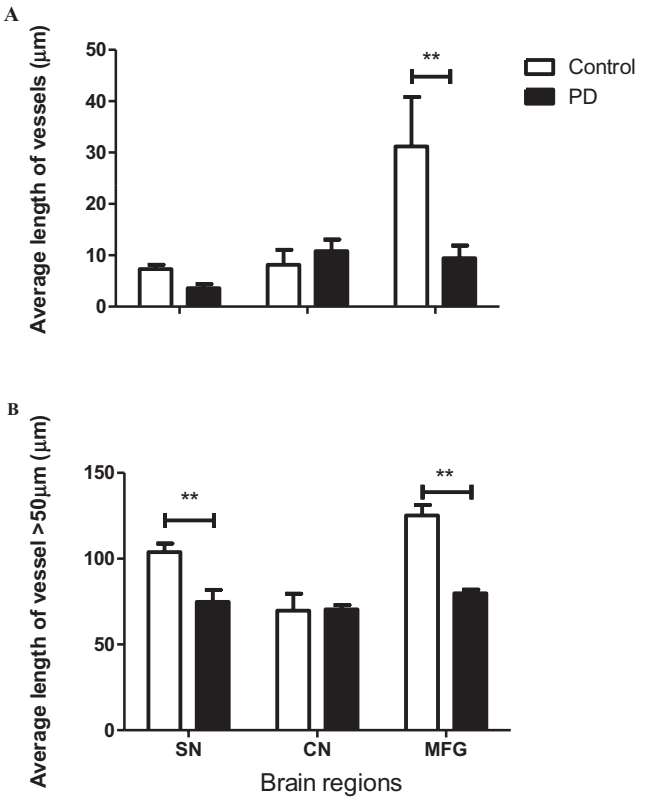

Figure 4. *Graphs show changes in average length of blood vessels*. Compared to the age-matched control cases ($n = 6$), the average length of vessels were significantly shorter in the MFG of PD cases (**A**, $n = 10$, $^{**}P < 0.01$) when the measurement included all vessels. The average length of the longer vessels (>50 μm) was significantly reduced in the SN and MFG of the PD cases compared to the control cases (**B**, $^{**}P < 0.01$). Data presented as mean ± SEM.

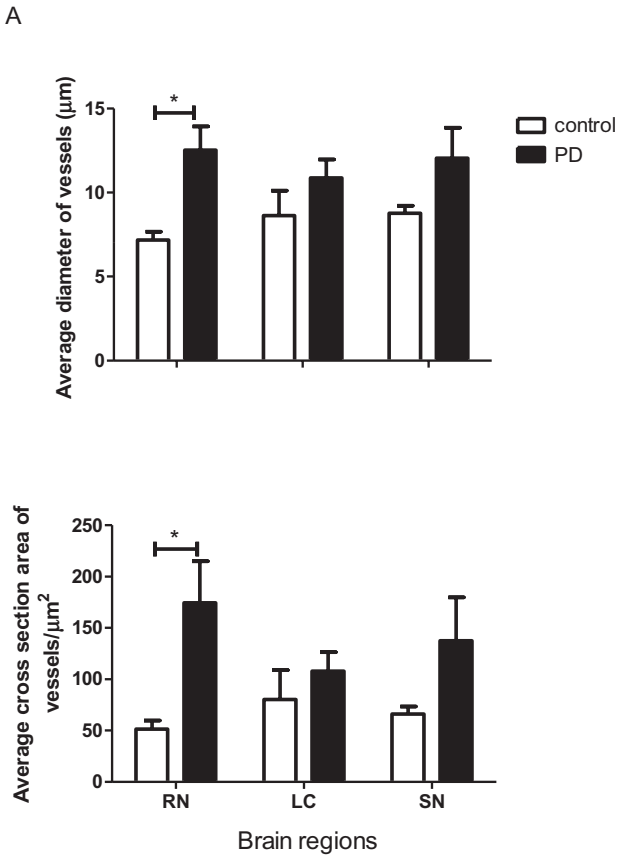

Figure 6. *Graphs show the changes in vessel size*. Compared to the control cases ($n = 4$), the average diameter (**A**) and the average cross-sectional area (**B**) of blood vessels were significantly increased in the RN of the PD cases ($n = 6$, $^{*}P < 0.05$). Data presented as mean ± SEM.

The vessel width was also analyzed by counting the number of small (diameter <10 μm) and larger (diameter >10 μm) vessels (Figure 7A,B), respectively. Compared to the controls, the number of small vessels was decreased in PD cases ($n = 6$, $P = 0.0003$, $F = 17.74$ [1,24], Figure 7A), whereas PD cases showed an increase in large vessels ($n = 6$, $P = 0.006$, $F = 8.87$ [1,24], Figure 7B). There was no difference between the brain regions examined and the difference between the groups was brain region dependent for the small vessels only. The post-test showed a significant decrease in small vessels in the LC ($P < 0.01$) and a significant increase in large vessels in the RN ($P < 0.05$), Figure 7A,B, respectively.

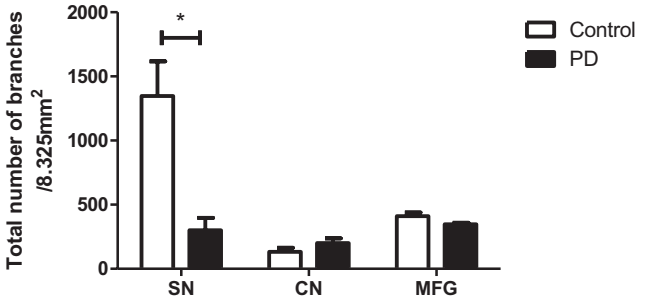

Figure 5. *Graph shows the number of branches of blood vessels*. The number of branches was significantly less in the SN of the PD cases compared to the age-matched control cases ($^{*}P < 0.05$). Data presented as mean ± SEM.

The ratio of small/large vessels was also analyzed. Compared to the control cases, the ratio of small/large vessels was significantly decreased in the PD cases ($n = 6$, $P < 0.0001$, $F = 24$ [1,24], Figure 7C). There was no difference between the brain regions, and the group effect was not brain region dependent. The post-test suggested a significant reduction of the ratio in the brain regions of the LC ($P < 0.05$) and RN ($P < 0.01$) (Figure 7C).

DISCUSSION

We have demonstrated, for the first time, vascular degeneration in human PD. The degenerative morphology includes the formation of endothelial "clusters," a damaged capillary network possibly due to vessel fragmentation and the loss of capillary connections.

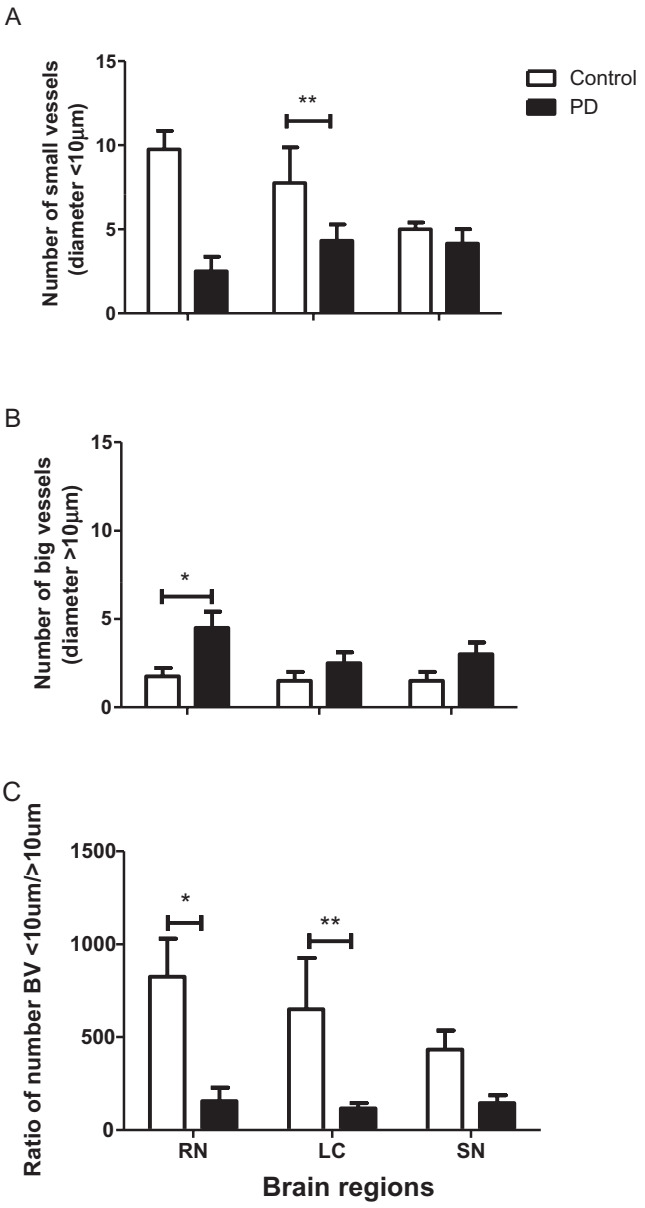

Figure 7. *Graphs show changes in vessel diameter*. The number of vessels with diameters smaller than 10 μm was reduced in the RN and LC of the PD cases (**A**, $n = 6$, $^{**}P < 0.01$), whereas the vessels with larger diameter (>10 μm) was increased in the RN of the PD cases (**B**, $^{*}P < 0.05$). There was a significant reduction in the ratio of small/larger vessels in the RN and LC (**C**, $^{*}P < 0.05$, $^{**}P < 0.01$, **C**), but not in the SN.

When compared to age-matched controls, the vessel size was larger in PD cases. Vessel degeneration was found in multiple brain regions, particularly in the SN, MFG and brain stem nuclei, but not in the CN. The data suggest that vascular degeneration may be an important additional contributing factor to the progress of PD, and may even be a contributor to the initial pathology that leads to neuronal degeneration.

The capillaries in the brain consist of the endothelial cells adjoined by tight junctions, the hydrophobic basal membrane, the pericytes and the astrocyte end feet in this order, from the blood to the tissue face (36) forming what is known as the blood-brain barrier (BBB). It differs from peripheral organs where the capillaries consist of a single layer of endothelial cells with leaky gaps between them (25). The BBB is able, for example, to restrict entry of polar molecules into the brain. Nutrients such as vitamins, glucose and amino acids cross the BBB using specific transporters (39), but peptides in general have limited ability to cross the BBB (41). Nonetheless, they can be transported into the brain via specific receptors expressed in brain endothelium under physiological or pathological conditions (40, 41).While we show in this manuscript a general loss of microvasculature that might contribute, at least during early stages, to vessel permeability, other mechanisms for transendothelial movement do exist.

Using factor VIII, a marker for the cytoplasm of endothelial cells, we found a significant amount of endothelial "clustering." Morphologically, factor VIII staining in the control cases was evenly distributed within the capillaries. In contrast, the factor VIII staining in PD capillaries was dense in some parts forming the "clusters" of various shapes and sizes with little or no staining between the "clusters." The most common feature of capillary "clusters" was the parallel lines that linked across the blood vessel walls. The mechanism of "cluster" formation however is not at all clear and needs to be further investigated. There was a small amount of endothelial "clustering" in the age-matched controls, but, by comparison, the amount and the percentage area of "clusters" were significantly increased in the PD cases. The data suggest that the formation of endothelial "clusters" was more specific to the PD and may be a contributing factor in the breakdown of the capillary network.

The integrity of the intact capillary network (bed) is essential for effective vascular function. Compared to the age-matched controls, we found that the capillaries in PD cases were shorter in average length, less in number, particularly those longer than 50 μm, and had fewer branches, suggesting the possibility of breakdown of the capillary network in PD cases. The vessel density was evaluated by measuring total vessel numbers, as well as selectively by number of longer vessels (>50 μm) in order to exclude fragmented capillaries. While the loss of vessel density in PD cases was highly significant in the SN across both measurements, the loss of vessels in the MFG of PD cases was only true for the longer vessels when compared to the age-matched controls. The data indicate that capillaries may be more fragmented in the frontal cortex of PD brains and that vessel degeneration is targeted to those longer capillaries. This interpretation was supported by the data obtained from measuring the average length of blood vessels. Compared to the age-matched control cases, the vessel length was shorter in the frontal cortex, but not in the SN in PD cases when measurements included all vessels. However, vessel length was significantly shorter in the SN of PD cases when measuring blood vessels longer than 50 μm.

The average size of a capillary is 5–10 μm in diameter. In a separate experiment, the changes in capillary size were also determined by measuring the diameter and the cross-sectional area of vessels in the SN, LC and RN. We found that the average diameter was less than 10 μm in the control cases, whereas the vessel diameter was larger (>10 μm) in PD cases, particularly in the

RN. A similar result was found when the vessel size was measured as the cross-sectional area of the vessels. Using 10 μm as a cutoff line for measuring the capillaries (<10 μm) and small arteries/veins (>10 μm), we found that the PD cases had fewer capillaries (in the RN) and more small arterioles/veins (in the LC) with a significant reduction in the ratio of small/large vessels throughout all nuclei. The data suggest that vessel degeneration in PD cases was primarily at the level of capillaries, which may themselves be more vulnerable to degeneration than the small arteries/veins, and/or to the enlarged capillaries as a result of vascular remodeling (27).

The transformation of the microvasculature from predominantly capillaries to predominantly small arterioles/venules has a profound effect on oxygen diffusion. Arterioles (and venules) are much larger vessels with, on average, three layers of endothelial cells as well as smooth muscle cells and pericytes (15). In normal tissue, the majority of oxygen diffusion occurs from the capillary vessels consisting of only one layer of endothelial cells (15). As a consequence of the loss of the capillary bed, tissues receive less oxygen leading to damage through processes such as the production of free radicals due to the inability to regenerate antioxidant enzymes, or insufficient oxygen available for oxidative metabolism.

The data presented here generated from two independent experiments tested the same hypothesis by measuring different parameters. These two methodology approaches generated data that were complementary to each other. The control cases in experiment 2 were not completely age-matched due to availability of the tissues in different brain regions.

Despite a uniform increase in endothelial "clusters" in the SN, CN and MFG of PD cases, the differences between the two groups with regard to vessel density, vessel length and vessel branches were only significant in some brain regions. While the loss of small vessels was consistent in the PD cases, changes of vessels in the age-matched controls varied, largely between the brain regions. This would suggest that the lack of difference between the groups was due to the age-related loss in vessel density, length and branches, which is brain region associated. For example, there was a consistent decrease in all parameters measured in the CN of the age-matched control cases compared to other brain regions. The age-related loss of brain vessels has been reported previously in aged brains (13). In addition to the hippocampus, the striatum is relatively more sensitive to age-related changes in structure (6, 19) and function (11), as well as other specific age-related clinical conditions (1). Thus, the vessel changes observed in the SN are likely to be more specific to PD pathology, while the loss of vessels in the CN may be a combination of the pathology of aging and PD. The frontal cortex, a brain region that is affected in PD, with Lewy Bodies present, may share a similar pathology with AD in terms of neuronal loss (17), and perhaps in vascular degeneration. Widespread cortical hypoperfusion has been reported at the early stage of PD (10).

Vascular remodeling and networking happens constantly even under conditions of neurodegeneration and insufficient vascular remodeling contributes to neuronal degeneration and functional decline. The changes in the vasculature of age-matched controls can be a complex mix of vessel degeneration associated with old age and vascular pathology as part of systemic vascular diseases as seen, for example, in hypertension, diabetes and obesity (11, 19). Thus, the interpretation of vascular changes in the senile brain is complicated and the data are difficult to interpret, which in turn makes the comparison with respect to young controls somewhat unreliable (31). Thus, we did not include a young control group in our study.

In addition to providing nutrients and taking metabolic wastes away, the function of capillaries in the brain is to serve as an impermeable barrier that protects our brain from peripheral harmful substances, for example, circulating pro-inflammatory factors. The disruption of the endothelial cells seen in the PD capillaries and pericyte deficiency seen in neurodegenerative conditions could mean the breakdown of the BBB (4, 8, 9) causing the accumulation of multiple peripheral neurotoxic molecules that contribute to neuronal dysfunction (4). It has been shown that apolipoprotein E4 activation of a pro-inflammatory CypA-nuclear factor-κB-matrix-metalloproteinase-9 pathway in pericytes mediates neurovascular injury, resulting in neuronal dysfunction and degeneration (5). As reported for AD and Amyotrophic Lateral Sclerosis, BBB disruption may play a vital role in PD (22), both pathologically and pharmacologically. 3,4-dihydroxyphenyl-L-alanine (L-DOPA) is the most widely used pharmacological agent for PD. Amino acid receptors (LAT), LAT1 that are expressed in the capillaries, transport L-DOPA across the BBB. The transport of L-DOPA may, for example, be lowered where there is microvessel loss, leading to the reduction of L-DOPA levels in the brain (20). It is now well known that the inflammatory response is elevated in the brain in neurodegenerative conditions, as this is now well recognized as a contributing factor to neuronal death. Even though we did not investigate the inflammatory response in the brains of our PD cases, the disrupted endothelial cells may indicate a potential pathway of entry and a subsequent role for an inflammatory response in PD.

Neurons, glial cells and endothelial cells also interact with each other and form a neuronal-glial-vascular unit both functionally and structurally (14, 24, 31, 36). The endothelial cells are involved in the process of neurogenesis by stimulating the self-renewal of neural stem cells, inhibiting their differentiation, and enhancing neuron production (33). Endothelial cells also produce neurotrophic factors, for example, vascular endothelial growth factor and nitric oxide synthase, which stimulate and regulate both neuronal survival and neuronal function (18). There are many neurotransmitters that regulate vascular functions (32, 35). Structurally, astrocytes, a glial phenotype, form part of the capillaries and, functionally, the glial-vascular interface is key to maintaining both neuronal and vascular functions in our brain. Although we did not examine the effect of endothelial degeneration on neuronal and glial function, vascular degeneration may well contribute to neuronal degeneration and inflammation in neurological conditions and vice versa. Understanding vascular degeneration is therefore critical if we are to interpret the neuronal–glial–vascular interaction, which has itself been suggested recently to be a novel target for therapeutic intervention (30).

REFERENCES

1. Abe Y, Yamamoto T, Soeda T, Kumagai T, Tanno Y, Kubo J *et al* (2009) Diabetic striatal disease: clinical presentation, neuroimaging, and pathology. *Intern Med* **48**:1135–1141.
2. Arganda-Carreras I, Fernández-González R, Muñoz-Barrutia A, Ortiz-De-Solorzano C (2010) 3D reconstruction of histological

sections: application to mammary gland tissue. *Microsc Res Tech* **73**:1019–1029.
3. Aston-Jones G, Shipley MT, Chouvet G, Ennis M, van Bockstaele E, Pieribone V *et al* (1991) Afferent regulation of locus coeruleus neurons: anatomy, physiology and pharmacology. *Prog Brain Res* **88**:47–75.
4. Bell RD, Winkler EA, Sagare AP, Singh I, LaRue B, Deane R, Zlokovic BV (2010) Pericytes control key neurovascular functions and neuronal phenotype in the adult brain and during brain aging. *Neuron* **68**:409–427.
5. Bell RD, Winkler EA, Singh I, Sagare AP, Deane R, Wu Z *et al* (2012) Apolipoprotein E controls cerebrovascular integrity via cyclophilin A. *Nature* **485**:512–516.
6. de Jong LW, Wang Y, White LR, Yu B, van Buchem MA, Launer LJ (2012) Ventral striatal volume is associated with cognitive decline in older people: a population based MR-study. *Neurobiol Aging* **33**:424. e10.
7. de Lau LM, Breteler MM (2006) Epidemiology of Parkinson's disease. *Lancet Neurol* **5**:525–535.
8. Desai Bradaric B, Patel A, Schneider JA, Carvey PM, Hendey B (2012) Evidence for angiogenesis in Parkinson's disease, incidental Lewy body disease, and progressive supranuclear palsy. *J Neural Transm* **119**:59–71.
9. Faucheux BA, Bonnet AM, Agid Y, Hirsch EC (1999) Blood vessels change in the mesencephalon of patients with Parkinson's disease. *Lancet* **353**:981–982.
10. Fernandez-Seara MA, Mengual E, Vidorreta M, Aznarez-Sanado M, Loayza FR, Villagra F *et al* (2012) Cortical hypoperfusion in Parkinson's disease assessed using arterial spin labeled perfusion MRI. *Neuroimage* **59**:2743–2750.
11. Guan J, Zhang R (2011) Age-related vascular degeneration and memory decline. In: The 10th International Conference on Alzheimer's and Parkinson's diseases Barcelona, Spain.
12. Halliday GM, Li YW, Blumbergs PC, Joh TH, Cotton RG, Howe PR *et al* (1990) Neuropathology of immunohistochemically identified brainstem neurons in Parkinson's disease. *Ann Neurol* **27**:373–385.
13. Hattiangady B, Shetty AK (2008) Aging does not alter the number or phenotype of putative stem/progenitor cells in the neurogenic region of the hippocampus. *Neurobiol Aging* **29**:129–147.
14. Hirase H (2005) A multi-photon window onto neuronal-glial-vascular communication. *Trends Neurosci* **28**:217–219.
15. Intaglietta M, Johnson PC, Winslow RM (1996) Microvascular and tissue oxygen distribution. *Cardiovasc Res* **32**:632–643.
16. Isaias IU, Marzegan A, Pezzoli G, Marotta G, Canesi M, Biella GE *et al* (2011) A role for locus coeruleus in Parkinson tremor. *Front Hum Neurosci* **5**:179, 1–9.
17. Iseki E (2004) Dementia with Lewy bodies: reclassification of pathological subtypes and boundary with Parkinson's disease or Alzheimer's disease. *Neuropathology* **24**:72–78.
18. Ishitsuka K, Ago T, Arimura K, Nakamura K, Tokami H, Makihara N *et al* (2012) Neurotrophin production in brain pericytes during hypoxia: a role of pericytes for neuroprotection. *Microvasc Res* **83**:352–359.
19. Jacobson J, Zhang R, Elliffe D, Chen K, Mathai S, McCarthy D *et al* (2008) Co-relation of cellular changes and spatial memory during aging in rats. *Exp Gerontol* **43**:928–938.
20. Kageyama T, Nakamura M, Matsuo A, Yamasaki Y, Takakura Y, Hashida M *et al* (2000) The 4F2hc/LAT1 complex transports L-DOPA across the blood-brain barrier. *Brain Res* **879**:115–121.
21. Kannurpatti SS, Motes MA, Rypma B, Biswal BB (2010) Neural and vascular variability and the fMRI-BOLD response in normal aging. *Magn Reson Imaging* **28**:466–476.
22. Kortekaas R, Leenders KL, van Oostrom JC, Vaalburg W, Bart J, Willemsen AT, Hendrikse NH (2005) Blood-brain barrier dysfunction in parkinsonian midbrain in vivo. *Ann Neurol* **57**:176–179.
23. Lindner MD, Cain CK, Plone MA, Frydel BR, Blaney TJ, Emerich DF, Hoane MR (1999) Incomplete nigrostriatal dopaminergic cell loss and partial reductions in striatal dopamine produce akinesia, rigidity, tremor and cognitive deficits in middle-aged rats. *Behav Brain Res* **102**:1–16.
24. Liu L, Su Y, Yang W, Xiao M, Gao J, Hu G (2010) Disruption of neuronal-glial-vascular units in the hippocampus of ovariectomized mice injected with D-galactose. *Neuroscience* **169**:596–608.
25. Mann GE, Zlokovic BV, Yudilevich DL (1985) Evidence for a lactate transport system in the sarcolemmal membrane of the perfused rabbit heart: kinetics of unidirectional influx, carrier specificity and effects of glucagon. *Biochim Biophys Acta* **819**:241–248.
26. Marchesi VT (2011) Alzheimer's dementia begins as a disease of small blood vessels, damaged by oxidative-induced inflammation and dysregulated amyloid metabolism: implications for early detection and therapy. *FASEB J* **25**:5–13.
27. Mattar EH, Haffor AS (2009) Effect of dobutamine and hyperoxia on free radicals production in relation to the ultrastructural alterations in the endothelial of myocardial capillary in rats, Rattus norvigicus. *Ultrastruct Pathol* **33**:209–215.
28. McMillan PJ, White SS, Franklin A, Greenup JL, Leverenz JB, Raskind MA, Szot P (2011) Differential response of the central noradrenergic nervous system to the loss of locus coeruleus neurons in Parkinson's disease and Alzheimer's disease. *Brain Res* **1373**:240–252.
29. Poewe W (2009) Treatments for Parkinson disease—past achievements and current clinical needs. *Neurology* **72**(Suppl 7):S65–S73.
30. Quaegebeur A, Lange C, Carmeliet P (2011) The neurovascular link in health and disease: molecular mechanisms and therapeutic implications. *Neuron* **71**:406–424.
31. Rodriguez JJ, Olabarria M, Chvatal A, Verkhratsky A (2009) Astroglia in dementia and Alzheimer's disease. *Cell Death Differ* **16**:378–385.
32. Sharp SI, Francis PT, Elliott MS, Kalaria RN, Bajic N, Hortobagyi T, Ballard CG (2009) Choline acetyltransferase activity in vascular dementia and stroke. *Dement Geriatr Cogn Disord* **28**:233–238.
33. Shen Q, Goderie SK, Jin L, Karanth N, Sun Y, Abramova N *et al* (2004) Endothelial cells stimulate self-renewal and expand neurogenesis of neural stem cells. *Science* **304**:1338–1340.
34. Waldvogel HJ, Curtis MA, Baer K, Rees MI, Faull RLM (2007) Immunohistochemical staining of post-mortem adult human brain sections. *Nat Protocols* **1**:2719–2732.
35. Wang P, Xie ZH, Guo YJ, Zhao CP, Jiang H, Song Y *et al* (2011) VEGF-induced angiogenesis ameliorates the memory impairment in APP transgenic mouse model of Alzheimer's disease. *Biochem Biophys Res Commun* **411**:620–626.
36. Wolburg H, Noell S, Mack A, Wolburg-Buchholz K, Fallier-Becker P (2009) Brain endothelial cells and the glio-vascular complex. *Cell Tissue Res* **335**:75–96.
37. Zarow C, Lyness SA, Mortimer JA, Chui HC (2003) Neuronal loss is greater in the locus coeruleus than nucleus basalis and substantia nigra in Alzheimer and Parkinson diseases. *Arch Neurol* **60**:337–341.
38. Zlokovic BV (2011) Neurovascular pathways to neurodegeneration in Alzheimer's disease and other disorders. *Nat Rev Neurosci* **12**:723–738.

39. Zlokovic BV, Apuzzo ML (1997) Cellular and molecular neurosurgery: pathways from concept to reality—part I: target disorders and concept approaches to gene therapy of the central nervous system. *Neurosurg* **40**:789–803. discussion 4.
40. Zlokovic BV, Mackic JB, Djuricic B, Davson H (1989) Kinetic analysis of leucine-enkephalin cellular uptake at the luminal side of the blood-brain barrier of an in situ perfused guinea-pig brain. *J Neurochem* **53**:1333–1340.
41. Zlokovic BV, Segal MB, Begley DJ, Davson H, Rakic L (1985) Permeability of the blood-cerebrospinal fluid and blood-brain barriers to thyrotropin-releasing hormone. *Brain Res* **358**: 191–199.